EJN European Journal of Neuroscience

FENS Federation of European Neuroscience Societies

European Journal of Neuroscience, pp. 1–11, 2015 doi:10.1111/ejn.12846

Hemispheric lateralization in top-down attention during spatial relation processing: a Granger causal model approach

N. W. Falasca,[1] S. D'Ascenzo,[2] A. Di Domenico,[3] M. Onofrj,[4] L. Tommasi,[3] B. Laeng[5] and R. Franciotti[4,6]
[1]BIND – Behavioral Imaging and Neural Dynamics Center, University of Chieti-Pescara, Chieti, Italy
[2]University of Modena and Reggio Emilia, Reggio Emilia, Italy
[3]Department of Psychological Science, Humanities and Territory, University of Chieti-Pescara, Chieti, Italy
[4]Department of Neuroscience, Imaging and Clinical Sciences, University of Chieti-Pescara, Chieti, Via dei Vestini 33, 66013 Chieti, Italy
[5]Department of Psychology, University of Oslo, Oslo, Norway
[6]ITAB, "G. d'Annunzio" University Foundation, Chieti, Italy

Keywords: attention window, causal information, hemispheric specialization, large and small cue, magnetoencephalography

Abstract

Magnetoencephalography was recorded during a matching-to-sample plus cueing paradigm, in which participants judged the occurrence of changes in either categorical (CAT) or coordinate (COO) spatial relations. Previously, parietal and frontal lobes were identified as key areas in processing spatial relations and it was shown that each hemisphere was differently involved and modulated by the scope of the attention window (e.g. a large and small cue). In this study, Granger analysis highlighted the patterns of causality among involved brain areas – the direction of information transfer ran from the frontal to the visual cortex in the right hemisphere, whereas it ran in the opposite direction in the left side. Thus, the right frontal area seems to exert top-down influence, supporting the idea that, in this task, top-down signals are selectively related to the right side. Additionally, for CAT change preceded by a small cue, the right frontal gyrus was not involved in the information transfer, indicating a selective specialization of the left hemisphere for this condition. The present findings strengthen the conclusion of the presence of a remarkable hemispheric specialization for spatial relation processing and illustrate the complex interactions between the lateralized parts of the neural network. Moreover, they illustrate how focusing attention over large or small regions of the visual field engages these lateralized networks differently, particularly in the frontal regions of each hemisphere, consistent with the theory that spatial relation judgements require a fronto-parietal network in the left hemisphere for categorical relations and on the right hemisphere for coordinate spatial processing.

Introduction

Our ability to encode spatial relations relies on at least two separate types of representation (Kosslyn, 1987, 1994). One is based on a quantitative parsing of space (e.g. 'how far' or 'how large' is something) and is called 'coordinate', the other, labelled 'categorical', parses space in a qualitative manner (e.g. whether something 'is to the left' or 'is above'). Neural and computational architecture has been proposed (Kosslyn *et al.*, 1989; Laeng, 2013; van der Ham *et al.*, 2014), suggesting that the two brain hemispheres can represent in parallel space – a predominantly right-hemispheric mode that assesses coordinate (or analog) spatial relations (e.g. the distance between two objects) and a predominantly left-hemispheric mode that assesses categorical (or digital) spatial relations (e.g. whether two objects are attached to one another, or one is above or below the other).

Several neuroimaging studies have recently provided converging evidence on the spatial function of such subsystems (Baciu *et al.*, 1999; Slotnick & Moo, 2006). Studies suggest that both parietal lobes play a key role in the perception of spatial relations (Slotnick *et al.*, 2001; Laeng *et al.*, 2002; Trojano *et al.*, 2006; Amorapanth *et al.*, 2010) and left and right prefrontal cortex show activity when categorical or coordinate respectively is held in memory (Kosslyn *et al.*, 1998; Trojano *et al.*, 2002).

Separate categorical and coordinate systems have also been implemented in computational networks that simulate spatial processing (Kosslyn & Jacobs, 1994), reporting that networks trained to make a categorical or a coordinate judgment more effectively for the former type if they receive their input from units with small, non-overlapping, receptive fields, as opposed to units with large, overlapping receptive fields, that help instead to facilitate the encoding of the latter type of spatial relation (Jacob & Kosslyn, 1994). Consistently,

Correspondence: Dr R. Franciotti, [4]Department of Neuroscience, Imaging and Clinical Sciences, as above.
E-mail: raffaella.franciotti@itab.unich.it

Received 23 September 2014, revised 16 December 2014, accepted 31 December 2014

Laeng *et al.* (2011) showed that encoding different types of spatial relations is modulated by manipulation of the scope of the attention window (Okubo *et al.*, 2010; Michimata *et al.*, 2011).

Recently, a magnetoencephalography (MEG) study (Franciotti *et al.*, 2013a) found neural evidence of the behavioural results, supporting the hypothesis that narrowing the attention window benefits the encoding of categorical relations, whereas spreading it promotes the encoding of coordinate relations. Activation of the frontal lobes indicates that each hemisphere has the ability to encode and judge both types of spatial relation as well as to narrow or expand the focus of attention, but that each can do so with different degrees of proficiency. Following from these previous results, the present study aims to highlight the possible causal interactions across brain areas involved during the processing of categorical and coordinate spatial relations by means of Granger causality (GC) analysis (Granger, 1969).

Specifically, we aimed to investigate whether the top-down mechanisms of attention could be related to information flow exchange from frontal areas towards visual occipital and parietal cortex and whether the facilitation process of the different scopes of attention on categorical or coordinate relations could be mediated by different causal connections among the brain areas involved.

Methods

Recordings and stimulation protocol

MEG recordings were carried out in 22 right-handed participants (12 females, mean age 26 ± 3 years, ranging from 21 to 33 years). All subjects signed a written informed consent before recording; the experimental procedures were carried out according to the *Declaration of Helsinki* and they were previously approved by the local Institutional Ethics Committee (at the University of Chieti-Pescara, Italy). MEG signals were bandpass filtered at 0.16–250 Hz and recorded at 1025 Hz sampling rate using 153 DC SQUID integrated magnetometers arranged on a helmet surface covering the whole head and 12 reference channels (Della Penna *et al.*, 2000). High-resolution whole head magnetic resonance imaging (MRI) was performed via a Philips scanner at 3 T using a 3D T1-TFE sequence. This was used to co-register MEG functional data with MRI anatomical images transformed into stereotaxic coordinates of the Talairach space.

The experimental task, using the same stimuli and procedure as in previous studies (Okubo *et al.*, 2010; Laeng *et al.*, 2011; Franciotti *et al.*, 2013a), consisted in comparing a sample stimulus and a subsequently presented matching stimulus appearing in one of the four possible quadrants of the screen (Fig. 1). Both types of stimuli included images of a pair of animals already used in previous studies (Laeng, 1994, 2006; Laeng *et al.*, 2011). Three possible pairing conditions of the same animals were used to create matching stimuli – coordinately different, categorically different and with no change in spatial relations. For the 'coordinately different' condition (COO), the distance between the two animals decreased in comparison to the sample stimulus while their relative orientation remained unchanged. For the 'categorically different' condition (CAT), the facing direction of one of the animals was reversed in comparison with the sample while the distance between animals remained unchanged. For the 'no change' condition (NoCh), the matching stimulus was exactly the same as the sample stimulus. Grey squares, slightly darker than the white background of the screen, came in two sizes, referred to as either 'large' or 'small' and were equally and randomly distributed across the experiment. These were used as cues to shift and modify the size of the attention window, so they were non-predictive of the task. In the cue-valid trials, cue location was superimposed to the to-be-presented location of the matching stimulus. In the cue-invalid condition, the cue and the match were located in different positions in the same trial. Cue-valid and cue-invalid trials were presented with a ratio of 9–1 for a total of 336 trials. At the beginning of each trial, a fixation cross was presented in the centre of the screen for 500 ms. Next, a sample stimulus appeared for 2000 ms, followed by

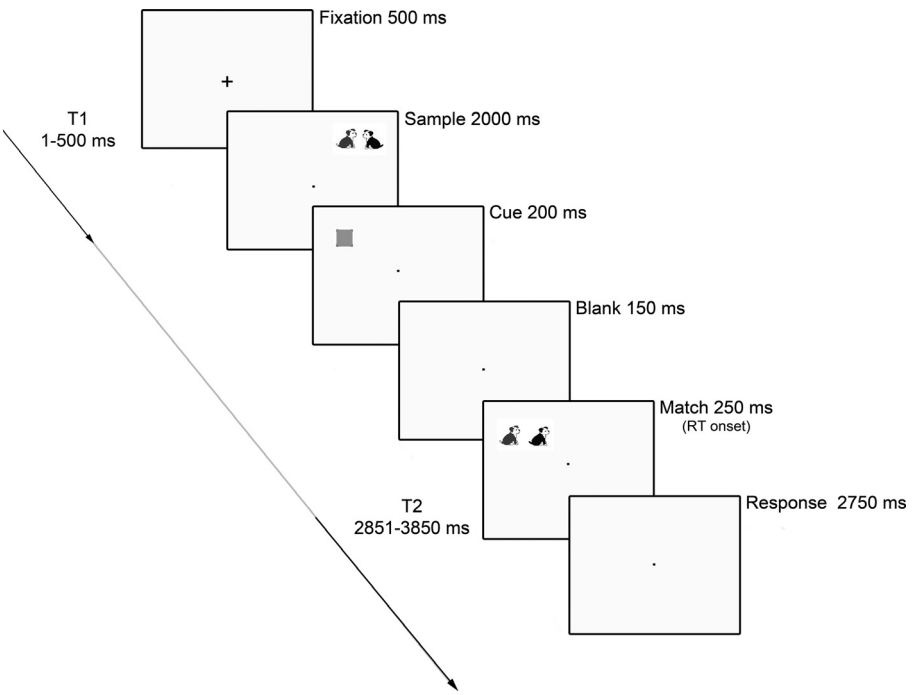

FIG. 1. Example of a valid trial for the CAT condition preceded by a small size cue (Small-CAT) with the two time intervals (T1, T2) used in the GC analysis.

the cue (for 200 ms). Immediately after the cue, the screen turned blank for 150 ms, followed by a matching stimulus presented for 250 ms. Each participant was trained to respond as fast and accurately as possible after the presentation of the matching stimulus indicating whether it was the same as the sample stimulus or different from it.

Figure 1 shows the presentation sequence and the time intervals (500 ms long) used for the GC analysis.

Preliminary MEG data analysis

Cardiac and ocular activities were monitored by means of bipolar electrodes placed on the chest and on the peri-orbital region to filter out possible heart-related contaminations on the MEG raw signals and to exclude from the analysis trials including eye movements from the fixation point. Heart-related contaminations were filtered out on the MEG raw signals by means of an adaptive algorithm using orthogonal projections (Samonas *et al.*, 1997; Della Penna *et al.*, 2004). The total number of noisy trials which were rejected was lower than 5% for each participant (See Fig. 2).

For each of the 12 experimental conditions (2 visual field presentation, left/right × 2 cue size, large/small × 3 spatial relations, CAT/COO/NoCh), we averaged the evoked magnetic fields of valid trials with correct responses over the timeline, from 0 ms (i.e. the matching stimulus onset) to 1000 ms (i.e. the maximal response time over which the behavioural responses were given on average). For each channel, a baseline level was computed as the mean value of the magnetic field in the time interval 0–1000 ms.

Generators of MEG-evoked responses were obtained for each of the experimental conditions by means of LORETA (low-resolution brain electromagnetic tomography analysis) (Pascual-Marqui *et al.*, 2002) as it was previously applied on the same data (Franciotti *et al.*, 2013a). Eight clusters of activations common to all conditions and that were also implicated in previous positron emission tomography and functional MRI studies on spatial relations (Kosslyn *et al.*, 1998; Slotnick & Moo, 2006) were selected from the activation maps of the CAT, COO and NoCh conditions. From each cluster of activation, we selected a region of interest (ROI) including the voxel of maximal activity and the 26 nearest neighbour voxels. The clusters of activation were – left and right visual cortex (LVC, RVC), left and right superior parietal lobe (LSPL, RSPL), left and right inferior parietal lobe (LIPL, RIPL) and left and right middle frontal gyrus (LMFG, RMFG). Equivalent current dipoles (ECDs) were then positioned in the centre of each of the eight clusters of activation (See Fig. 2). To evaluate the orientation of each dipole we first determined objectively the time interval of the maximal

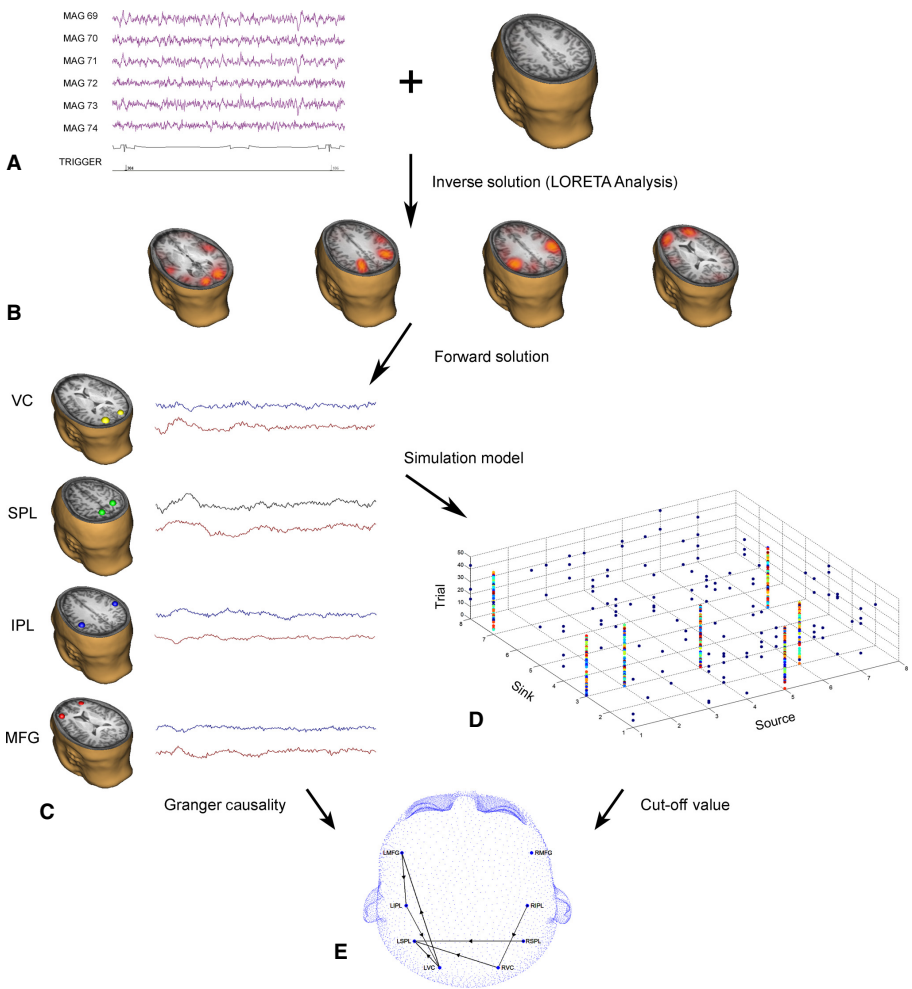

FIG. 2. Schematic representation of data analysis. (A) Traces of MEG raw data and structural MRI used for the localization of the sources. (B) Cluster of activations provided by LORETA. (C) Equivalent current dipoles located at the centre of the clusters and source waveforms over time estimated by the forward solution. (D) 3D matrix from simulation – GC values for each trial. (E) GC results on a head model.

activity for each source by a data-driven statistical approach. The intensity strength (nA.m/cm^3) of each ROI was averaged across all conditions (discarding type of spatial relations, cue size and visual field of presentation). Thus, the mean intensity of each ROI was computed across 50-ms time intervals and normalized to the maximal value obtained for each subject among the 20 time intervals to eliminate inter-
subject variability on source strength.

For each cluster, we performed one-way analysis of variance (ANOVA) for each ROI separately on normalized intensity strength with 20 temporal intervals of 50 ms as main factor, to obtain the time intervals in which the source activities were higher than all the rest of the epoch. Then, for each condition, the orientations of the eight ECDs were estimated by means of a multiple source analysis based on genetic algorithm provided by the BESA software (Megis, Gräfelfing, Germany) to model the involved sources. The fitting intervals for each dipole are shown in Table 1. The estimated orientations of the dipoles are typically influenced by MEG technique, which is mainly sensitive to tangentially orientated sources and theoretically silent to radially dipole sources.

After identification of the positions and orientations of the eight dipolar sources, the source waveforms describing their amplitude over time were obtained across all trials throughout the whole recording session by applying an inverse operator to the instantaneous raw magnetic field distribution over the helmet (Della Penna *et al.*, 2004). The activations of each source were estimated with 0.97 ms (1/1025 Hz) temporal resolution.

GC analysis was then applied on the eight ECD waveforms for each single trial for the time intervals T1 (1–500 ms, fixation) and T2 (2851–3350 ms, presentation of the match stimulus). Specifically, to evaluate the temporal dynamics of the connectivity pattern during and after the presentation of the match stimulus we used for T2 20 sliding windows, with 450 ms of overlap (each 500 ms long) from the onset of the match stimulus to 1000 ms after the presentation of the match stimulus.

For each condition, valid trials with correct responses were selected for GC analysis.

GC analysis

GC analysis was employed to identify patterns of causal interaction between sources. Data analysis was performed using home-made software, BSMART, a MATLAB/C Toolbox implemented to analyse brain circuits (Cui et al., 2008) and GC connectivity analysis (Seth, 2010).

The probabilistic concept of GC is based on the idea that causes precede their effects in time. According to linear vector autoregressive (VAR) models, the time series $X_1(t)$ and $X_2(t)$ can be explained by their own past by means of a linear model with coefficients a_j and b_j and prediction errors ε_1 and η, respectively:

$$X_1(t) = \sum_{j=1}^{m} a_j X_1(t-j) + \varepsilon_1(t),$$

$$X_2(t) = \sum_{j=1}^{m} b_j X_2(t-j) + \eta_1(t).$$

Lagged VAR models are used to determine the ability of one time-varying signal to predict the future behaviour of another, comparing the accuracy of the prediction obtained by considering only information of its own past with inclusion of the past of the other signal of the system (Granger, 1969). Thus, the temporal dynamics of the time series $X_1(t)$ and $X_2(t)$ (both of length T) can be described also including in the model not only information on the own past of the time series, but also information on the past of the other time series, with prediction errors $\varepsilon_2(t)$ and $\eta_2(t)$, which are different from the previous $\varepsilon_1(t)$ and $\eta_1(t)$:

$$X_1(t) = \sum_{j=1}^{m} a_j X_1(t-j) + \sum_{j=1}^{m} b_j X_2(t-j) + \varepsilon_2(t),$$

$$X_2(t) = \sum_{j=1}^{m} c_j X_2(t-j) + \sum_{j=1}^{m} d_j X_1(t-j) + \eta_2(t),$$

where m is the maximum number of lagged observations included in the model (the model order, $m << T$), whereas b and d are the gain factors, respectively, of the signal X_2 (source) influencing the signal X_1 (sink), and of the signal X_1 (source) influencing the signal X_2 (sink).

The linear influence ($F_{X_1 \to X_2}$) from $X_1(t)$ to $X_2(t)$ and ($F_{X_2 \to X_1}$) from $X_2(t)$ to $X_1(t)$ can be calculated as the ratio between the variances of the residual errors.

$$F_{X_1 \to X_2} = \log\left(\frac{\mathrm{var}(\eta_1)}{\mathrm{var}(\eta_2)}\right),$$

$$F_{X_2 \to X_1} = \log\left(\frac{\mathrm{var}(\varepsilon_1)}{\mathrm{var}(\varepsilon_2)}\right).$$

GC analysis is generalized to the multivariate (conditional) case in which the G-causality of X_2 on X_1 is tested in the context of multiple additional variables X_3, …, X_n (Geweke, 1982) when all other variables X_3, …, X_n are also included in the regression model. In our data, a conditional multivariate VAR (MVAR) model was applied to the eight time series.

TABLE 1. The anatomical locations, Talairach and MNI coordinates of the centre of clusters as estimated by means of LORETA; for each region, fit intervals for the estimation of the dipole orientation are shown

	ECD position (mm)						
Region	Talairach			MNI			Fit interval (ms)
Visual cortex left	−22	−81	4	−22	−84	9	50–150
Visual cortex right	20	−83	1	23	−87	5	50–150
Left superior parietal lobe	−35	−53	35	−36	−51	40	50–400
Right superior parietal lobe	29	−60	33	33	−59	38	50–400
Left inferior parietal lobe	−49	−31	31	−51	−28	34	50–550
Right inferior parietal lobe	53	−31	31	59	−28	32	50–550
Left middle frontal gyrus	−31	46	10	−33	51	2	350–1000
Right middle frontal gyrus	32	46	10	36	52	1	350–1000

A crucial aspect of GC analysis regards the definition of the model order m and the number of time points T required to estimate causality. Indeed, a low order value can lead to a poor representation of the data, whereas a high value can lead to incorrectly rejected null hypotheses (type I errors). The Akaike information criterion (Akaike, 1974) was used to estimate the order of the model (Bressler & Seth, 2011) for each subject and for each trial separately. When the Akaike information criterion did not find a global minimum, the trial was discarded (about 3% of the total trials).

For the T1 time interval GC analysis was performed on all trials discarding the type of conditions resulting in one pattern of causal connection, whereas for the T2 time interval, 12 patterns of connectivity were estimated according to the 12 experimental conditions (2 visual field × 2 cue size × 3 spatial relations).

For each of the experimental trials, eight signals from eight ECD waveforms 512 time points long (T = 500 ms) were separately checked for covariance stationarity by using the Durbin–Watson test, based on MATLAB code provided by Seth (2010) and the Dickey–Fuller test ($P < 0.01$) to identify unit roots. The mean number across subjects of non-stationary trials compared with all trials was 60 ± 20 and 77 ± 14% for T1 and T2 time intervals, respectively. In cases where unit roots existed, we generated covariance stationarity using a first-order differencing applied to time series (Seth, 2005, 2010; Gow *et al.*, 2008). The consistency of the MVAR model, which ensures that the MVAR model properly represents the data, was verified by the tests proposed by Ding *et al.* (2000) and by the Durbin–Watson statistics, which assess whether the residuals are uncorrelated. The consistency values performed for each trial separately indicated whether there was a good correspondence between the real data and the MVAR model. Trials with model consistency lower than 80% were discarded. Then, a GC analysis was computed for each subject and each trial separately by a MATLAB toolbox for multi-trial data (Seth, 2010), obtaining a GC matrix of eight rows and eight columns of GC magnitude, representing the causal strength of the connection between each couple of nodes. The F-statistic, Bonferroni-corrected ($P < 0.05$), was applied to the logarithm of the GC magnitude matrix (Benjamini & Hochberg, 1995). The values of GC magnitude that did not reach the significance threshold were set to zero. Trials with all GC values equal to zero were discarded from subsequent analysis. To eliminate causal interactions with type I errors, we estimated by means of simulations (see below) the cut-off values of GC magnitude, and subsequently all GC values lower than the cut-off value were set to zero. Model order size and results from stationary and non-stationary trials were first compared and the results then merged. The model order size and the standard deviation across subjects were 20 ± 2 and 19 ± 2 for stationary and non-stationary trials, respectively, for the T1 and T2 temporal intervals.

For all subjects, the GC matrixes from each trial of the same condition were concatenated and a matrix containing the number of occurrences of connectivity from each pair of nodes (number of trials with non-zero GC magnitude between each pair of nodes) was computed. When the connectivity between two nodes (GC value different from 0) was found in a few subjects (lower than 80%), the value of GC for that connection was set to zero, otherwise the GC value for that connection was obtained from the mean of the GC values across all subjects. The final result is then a GC matrix with eight rows and eight columns containing the mean values of GC magnitude (causal strength) for each connection between nodes (See Fig. 2).

Simulations

A simulation analysis was performed to estimate cut-off values of data, which highlighted causal interactions without type I errors. The simulation was performed by means of Simulink MATLAB software and consisted of a network of sources and sinks that represent a reproduction of the recorded signals of the cerebral electric field (Blinowska *et al.*, 2010). We simulated sources and sinks which replicated the key features found in the real data (number of time series, signal length, frequencies, signal-to-noise ratio). The simulation included signals derived from algorithms containing Poisson random functions together with white and pink noise generators. In the connections between the different signals, delays and gains of the signals were also included. The main component of each simulated signal was the sum of the electric fields generated by the mean response of neuron populations. The validity of the simulation software was tested by means of different oscillatory signals according to the previous literature (Baccalà & Sameshima, 2001; Schelter *et al.*, 2005).

Generated signals were checked for similarity with real data by means of an output device provided by Simulink. Then, a GC analysis was performed on the simulated data. The best correspondence between the prediction of Granger analysis and the information flow exchanges imposed previously in the simulation allowed estimation of the minimum gain value of the source and the minimum number of trials needed to highlight causal relationships. Thus, for simulated data, GC analysis estimated the right direction of causal information without type I errors when the gain of the sources involved in the flow exchange was > 0.2 and the number of trials was > 300. Indeed, the simulation results showed that when a source influenced a sink with a gain < 0.2, the causal information was not detected by the Granger analysis and/or type I errors were evident.

Statistical comparisons

To describe the interactions between the eight brain regions of the network, we used the number of total connections of each node, and the in-degree and the out-degree of each node of the network. The in-degree in a GC causal connectivity network means the number of causal in-flow connections to the node from any of the other nodes in the network. Out-degree of a node means the number of causal out-flow connections from the node to any of the other nodes in the network (Jiao *et al.*, 2011).

For T1 and T2 temporal windows, the statistical comparison was performed on all subjects and successively the total group of subjects was divided into two subgroups based on behavioural results. Specifically, the median of the difference of the reaction times (RTs) between the CAT and COO conditions was used to divide the subjects into two subgroups of high vs. low performers. All subjects with this difference lower than the median value were considered high performers, and the other subjects were considered low performers.

For the T1 temporal window, within-subject statistical analyses were performed on in-degree and out-degree by means of ANOVA with two factors and eight conditions – ROIs (VC, SPL, IPL, MFG) and hemisphere (left, right). Then, ANOVA was repeated using low and high performers as categorical variables.

For the T2 temporal window, a four-way ANOVA was performed on the total causal connections with cue size (large, small), visual field of stimuli presentation (left, right), spatial relation (CAT, COO, NoCh) and time (20 sliding windows) as factors to test for possible differences in the number of connections across temporal windows.

Subsequently, for each of the 20 sliding windows of T2, within-subject statistical analyses were performed on the total number of causal connections, on in-degree and out-degree separately. For the comparison of the number of total connections, a three-way ANOVA was performed among 12 conditions – cue size (large, small), visual

field of stimuli presentation (left, right) and spatial relation (CAT, COO, NoCh). The in-degree and the out-degree of each node were compared by means of an ANOVA with five factors and 96 conditions – cue size, visual field, spatial relation, ROIs (VC, SPL, IPL, MFG) and hemisphere (left, right). A *post-hoc* analysis using the Duncan test was used for multiple comparisons. The level of statistical significance was set at 5% ($P < 0.05$). For each of the 20 sliding windows, the ANOVA was repeated using low and high performers as categorical variables. The Mauchly's test of sphericity was used to evaluate the sphericity assumption. If the sphericity assumption was violated, the Greenhouse–Geisser epsilon correction was used to adjust the degrees of freedom.

Results

Behavioural results

Both statistical analysis on response accuracy values and RT showed that participants were less accurate and slower for the CAT than both NoCh and COO spatial relations, reflecting the greater difficulty of the categorical spatial relation task than the other spatial relation tasks. In addition, participants were less accurate when they had to evaluate COO-small cue than COO-large cue trials and they were slower when matching stimuli were presented in the right than in the left visual field and when matching stimuli followed the small cue than the large cue. All statistical results were shown in detail in a previous paper (Franciotti *et al.*, 2013a).

GC results

For time series that were not stationary, one application of differencing was sufficient to obtain stationary time series. GC results obtained from the first-order differencing of the non-stationary time series were compared with the GC results from the stationary time series. The comparison on the model order size and on the number of connections showed no difference between the two approaches.

Table 2 shows all significant effects for in-degree and out-degree during the T1 temporal interval. In particular, statistical analyses on T1 showed a different involvement of the left and the right hemisphere and significant differences across ROIs. The number of in-degrees was higher in the left than in the right hemisphere and the number of out-degrees was higher in the right than the left hemisphere, indicating that the right hemisphere could be considered the source of the causal information. The significant main effect of the ROIs showed a lower connectivity in MFG than the other ROIs and VC was more involved as a source than the other ROIs. No difference was found between the two subgroups of subjects, indicating that behavioural results were not linked to the connectivity pattern of the beginning of the task. Figure 3A shows the casual flows among brain areas for T1 temporal interval.

GC analyses were conducted over sliding time intervals to understand the time course of the connectivity pattern during the T2 temporal interval. For the comparison of the total number of connections across time, the four-way ANOVA showed no significant differences for time factor ($P = 0.35$). Figure 3B and C show the casual flows among brain areas for the T2 temporal interval, from 450 to 950 ms after the onset of the match stimulus.

During T2 the left fronto-parietal connections were mainly involved during categorical spatial relations, whereas right fronto-parietal connections were found during coordinate spatial relations. The direction of causal information was from right middle frontal gyrus to parietal cortex (top-down mechanism) and from visual cortex to left middle frontal gyrus.

Statistical comparison of the total number of connections of the network for each temporal window showed significant effects for spatial relation from 100 to 600 ms ($F_{2,38} = 7.22$, $P < 0.005$), from 250 to 750 ms ($F_{2,38} = 3.97$, $P < 0.05$) and from 300 to 800 ms ($F_{2,38} = 4.01$, $P < 0.05$) after match stimulus presentation. The number of connections was lower during CAT than COO and NoCh conditions ($P < 0.05$ for all comparisons). Visual field presentation was also significant for 100–600 ms ($F_{1,19} = 10.08$, $P < 0.005$) and 300–800 ms ($F_{1,19} = 4.61$, $P < 0.05$) showing a larger number of

TABLE 2. Significant statistical results on in-degree and out-degree connections for the T1 temporal window

Flux	Significant effects	*F*	*P*	*Post-hoc* comparison	*P*
In-degree	ROIs	18.53	0.000	SPL > VC, IPL	0.04
				SPL > MFG	0.000
				VC > MFG	0.000
	Hem	12.93	0.002	Left > Right	0.002
	ROIs × Hem	8.38	0.000	LSPL > LVC	0.000
				LVC > LMFG	0.005
				RVC > RMFG	0.000
				LSPL > RSPL	0.000
				LSPL > LIPL	0.001
				LSPL > LMFG	0.000
				RSPL > RMFG	0.003
				RIPL > RMFG	0.01
Out-degree	ROIs	14.73	0.000	VC > IPL, MFG	0.000
				VC > SPL	0.005
				SPL > MFG	0.001
				IPL > MFG	0.02
	Hem	13.2	0.002	Right > Left	0.002
	ROIs × Hem	3.05	0.000	RVC > LVC	0.03
				LVC > LSPL, LIPL	0.001
				LVC > LMFG	0.000
				RVC > RIPL	0.01
				RVC > RMFG	0.000
				RSPL > LSPL, RMFG	0.000
				RIPL > LIPL, RMFG	0.004

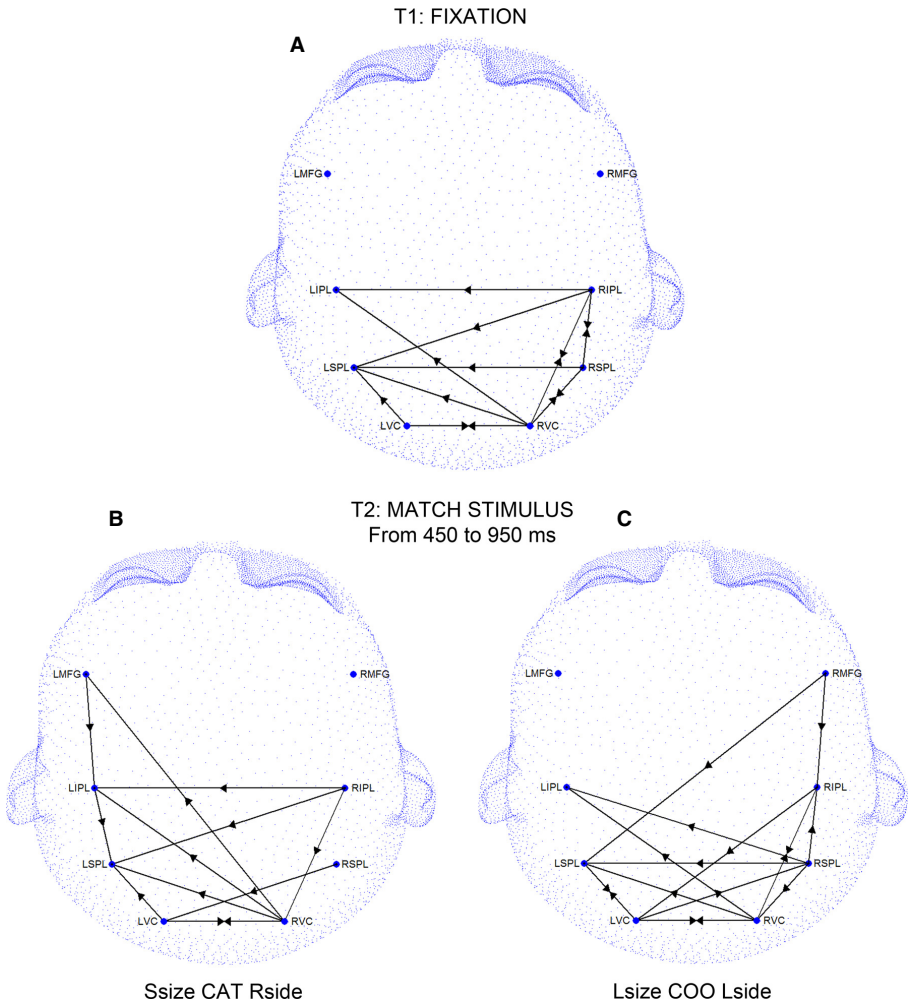

FIG. 3. GC patterns during T1 (A) and T2 temporal window from 450 to 950 ms after the onset of the match stimulus (B, C). Arrows indicate the direction of all statistically significant instances of GC. For T2, the pattern of connectivity is shown for categorical spatial relation attending to the right visual field, preceded by small cue (B, Ssize CAT Rside) and for coordinate spatial relation attending to the left visual field preceded by large cues (C, Lsize COO Lside). Note the involvement of the left and right fronto-parietal connections during categorical and coordinate spatial relation. respectively.

connections when the match stimulus was presented on the left than on the right side.

In-degree

ANOVAS with five factors on in-degree (sinks) showed main significant effects for ROIs and hemisphere for all sliding windows. All significant values for all sliding windows are reported in Table 3. The number of connections was highest in SPL, decreasing statistically in VC, IPL and MFG, and it was greater in the left than in the right hemisphere. The interaction ROIs × Hemisphere was also significant for all sliding windows, showing a greater number of connections for the left than for the right hemisphere in SPL and IPL.

When we included the subgroups analyses we also obtained a significant difference between the two subgroups, showing a greater number of in-flow connections for low than for high performers (Table 3). The interaction Cue size × Spatial relations × Hemisphere × Subgroups was significant for the following sliding windows – from 50 to 550 ms ($F_{2,36} = 3.41$, $P < 0.05$), from 350 to 850 ms ($F_{2,36} = 3.63$, $P < 0.05$), from 400 to 900 ms ($F_{2,36} = 3.51$, $P < 0.05$), from 450 to 950 ms ($F_{2,36} = 3.45$, $P < 0.05$) and from 500 to 1000 ms ($F_{2,36} = 4.19$, $P < 0.05$) after match stimulus presentation. Significant *post-hoc* comparisons for the sliding window from 500 to 1000 ms are reported in Table 4.

Out-degree

ANOVAS with five factors on out-degree (sources) showed significant main effects for cue size, spatial relations, ROIs and hemisphere. All significant values for all sliding windows are reported in Table 3. The number of out-degrees was lower for large cue than for small cue, was lower for CAT than for COO and NoCh spatial relations, was higher for VC than the other ROIs for all sliding windows and was lower for the left than for the right hemisphere. In addition the interaction ROIs × Hemisphere was also significant, showing that LVC and RVC were more involved as sources than the other ROIs, and VC, SPL and the IPL were more involved in the right than in the left hemisphere.

When we included the subgroups analyses, we also obtained a significant difference between the two subgroups, indicating a larger number of out-degree for low than for high performers (Table 3), a

TABLE 3. Significant main effects and interactions on in-degree and out-degree in all T2 temporal intervals

	In-degree				Out-degree					
Interval	ROIs $F_{3,57}$	Hemisphere $F_{1,19}$	ROIs × Hemisphere $F_{3,57}$	Low/High performers $F_{1,18}$	Cue size $F_{1,19}$	Spatial relation $F_{2,38}$	ROIs $F_{3,57}$	Hemisphere $F_{1,19}$	ROIs × Hemisphere $F_{3,57}$	Low/High performers $F_{1,18}$
0–500	14.4***	13.6***	8.3***	6.2*	n.s.	n.s.	17.1***	12.5**	3.4*	6.2*
50–550	14.7***	14.2***	10.4***	9.2**	5.9*	n.s.	11.6***	14.4***	n.s.	9.2**
100–600	17.5***	17.0***	8.6***	8.0**	n.s.	7.2**	14.0***	16.8***	3.1*	8.0**
150–650	12.7***	12.7***	6.6**	5.4*	n.s.	n.s.	21.4***	13.0***	3.1*	5.4*
200–700	14.9***	17.2***	5.3**	5.4*	n.s.	n.s.	16.9***	26.9***	n.s.	5.4*
250–750	17.4***	18.9***	7.5***	6.0*	n.s.	n.s.	16.9***	17.5***	2.9*	6.0*
300–800	12.0***	15.5***	6.2***	6.4*	n.s.	4.0*	12.8***	12.6**	n.s.	6.4*
350–850	13.1***	12.5***	4.8**	n.s.	n.s.	n.s.	22.6***	18.9***	3.2*	n.s.
400–900	12.5***	14.5***	5.7***	4.9**	n.s.	n.s.	19.4***	17.1***	2.7*	4.9*
450–950	12.6***	12.4**	8.8***	n.s.	n.s.	n.s.	20.4***	19.2***	3.4*	n.s.
500–1000	10.5***	17.9***	7.1***	n.s.	n.s.	n.s.	21.0***	21.5***	n.s.	n.s.
550–1050	8.9***	20.9***	8.4***	5.8**	n.s.	n.s.	15.2***	16.2***	4.1**	5.8*
600–1100	11.9***	18.7***	6.3***	6.3*	n.s.	n.s.	12.6***	15.1***	3.2*	6.3*
650–1150	15.1***	16.2***	9.0***	n.s.	n.s.	n.s.	13.4***	14.7***	n.s.	6.0*
700–1200	14.9***	18.6***	6.3***	n.s.	n.s.	n.s.	12.2***	11.3**	n.s.	n.s.
750–1250	16.6***	14.0***	10.4***	5.9*	n.s.	n.s.	12.2***	11.9**	n.s.	5.9*
800–1300	12.5***	14.7***	7.8***	5.8*	n.s.	n.s.	12.0***	16.0***	3.8*	5.9*
850–1350	14.5***	18.6***	5.1***	n.s.	n.s.	n.s.	11.8***	12.5**	3.2*	n.s.
900–1400	14.7***	8.9***	8.2***	n.s.	n.s.	n.s.	14.4***	13.2***	3.4*	n.s.
950–1450	13.0***	8.6***	11.1***	n.s.	n.s.	3.8*	15.6***	10.6**	3.6*	n.s.
0–1450	15.9***	19.4***	8.9***	5.3*	n.s.	n.s.	18.0***	16.3***	3.5*	5.3*

*$P < 0.05$, **$P < 0.01$, ***$P < 0.001$.

significant interaction Cue size × Spatial relation × Hemisphere × Subgroups ($F_{2,36} = 4.26$, $P < 0.05$) for the window from 700 to 1200 ms after match stimulus presentation. Table 4 shows all *post-hoc* significant results for this interaction.

Discussion

Previous neuroimaging studies reported that SPL, IPL and MFG are implicated in different visuospatial tasks (Corbetta *et al.*, 1998; Rosen *et al.*, 1999) and specifically in spatial relation processing (Kosslyn *et al.*, 1998; Slotnick & Moo, 2006; Franciotti *et al.*, 2013a). Our MEG data allowed us to reveal the involvement of a specific network that is active during the processing of spatial relations of the categorical vs. coordinate types. Specifically, VC, SPL and RIPL are interconnected during the entire duration of the task. In particular, RVC, RSPL and RIPL seem to play a central role in the information flow from fixation for the whole duration of the trial (Fig. 3). The total number of connections was not statistically different across temporal windows of T2, indicating that the number of directed influences was not modified during processing of the task. Indeed, T2 represents the temporal windows from the onset of the match stimulus to the following 1000 ms that corresponds, approximately, to the average RT (Franciotti *et al.*, 2013a). Another possible explanation is that the possible changes across times were hidden by the temporal windows of 500 ms length.

The present results support the idea that top-down mechanisms involved in endogenous orientating of attention are generated in the frontal cortex, as has been previously reported in visual attention tasks (Desimone & Duncan, 1995; Kastner & Ungerleider, 2000; Corbetta & Shulman, 2002; Moore *et al.*, 2003; Serences & Yantis, 2006). Specifically, our results reveal a causal information flow from the right middle frontal gyrus to parietal and visual cortex (Fig. 3B), and thus the frontal area seems to exert top-down modulatory influence on the visual and parietal cortex, but only in the right hemisphere. For the left hemisphere the direction of causal information flow runs in the opposite direction, from the parietal and visual cortex to the left middle frontal gyrus, supporting the idea that in this paradigm the top-down signals are selectively related to the right hemisphere (Fig. 3C).

The modulation of information flow by manipulation of the scope of the attention window was tested by statistical comparison of the total number of connections and of in-degree and out-degree. Thus, these results indicate that the source of information exchange is in the right hemisphere for all conditions and the left middle frontal gyrus is selectively involved when solving the categorical spatial judgment.

A smaller number of connections was found during the more difficult task. Indeed, a smaller number of connections was found in CAT than COO and NoCh and when the match stimulus was presented in the right than in the left visual field. The decreased functional connectivity may represent increased efficiency of the functional network (Yoo *et al.*, 2013), i.e. when the task is more demanding (CAT condition, attended stimulus in the right visual field).

The comparison between high and low performers indicated that the latter had more connections than the former and more in-flow and out-flow, possibly indicating that the network is less efficient. The increased functional connectivity in low performers could be related to their lower ability to keep relevant information in mind and ignore irrelevant information (Bunge *et al.*, 2001).

In addition, in high performers the benefit of the small cue preceding the CAT condition was related to lower in-flow connections in the left hemisphere than for the large cue condition, whereas the NoCh condition showed lower in-flow connection when it was preceded by the large cue. These results showed that a better performance (i.e. the RTs during the more difficult task, CAT, were similar to those of the easier task, COO) was obtained when the

TABLE 4. Significant statistical results on in-degree and out-degree connections in the interaction Subgroup × Cue size × Spatial relation × Hemisphere for the T2 temporal interval; the most important statistical findings are shown in bold

	Low/high performers × cue size × spatial relation × hemisphere		
Flux		*Post-hoc* comparison	*P*
In-degree sliding window from 500 to 1000 ms	In low performers	Small CAT Right < Large CAT Right	0.036
		Small CAT Left > Small CAT Right	0.000
		Small CAT Left > Large CAT Left	0.033
		Large CAT Left > Large CAT Right	0.013
		Large COO Left > Large COO Right	0.05
		Large COO Left < Small COO Left	0.039
		Large NoCh Left > Small NoCh Left	0.046
		Large NoCh Right > Small NoCh Right	0.021
		Large NoCh Left > Large NoCh Right	0.043
		Small NoCh Left > Small NoCh Right	0.02
	In high performers	Large CAT Left > Large CAT Right	0.012
		Small CAT Left < Large CAT Left	0.026
		Small COO Left > Small COO Right	0.022
		Large NoCh Left < Small NoCh Left	0.004
		Small NoCh Left > Small NoCh Right	0.001
Out-degree sliding window from 700 to 1200 ms	In low performers	**Small CAT Right < Large CAT Right**	0.014
		Large CAT Left < Large CAT Right	0.01
		Large NoCh Left > Small NoCh Left	0.016
		Small NoCh Left < Small NoCh Right	0.05
	In high performers	Large CAT Left < Large CAT Right	0.035
		Small CAT Left < Small CAT Right	0.002
		Small COO Left < Small COO Right	0.011
		Large NoCh Left < Large NoCh Right	0.038
		Small NoCh Left < Small NoCh Right	0.029

hemisphere specialized in the task (e.g. the left hemisphere for the CAT condition) receives less information. The benefit of the small cue in the CAT condition was also evident in the out-flow connection and the right hemisphere appears to transfer less causal flow when a cue is small than when it is large.

For the low performers, when the CAT condition was preceded by the small cue, the left hemisphere received more information flow than when it was preceded by the large cue, suggesting that the network is less efficient. For the COO condition, the left hemisphere received less causal connection when it was preceded by the large than the small cue, in agreement of the benefit of the large cue for the coordinate spatial judgment.

In conclusion, this study, using for the first time GC on the processing of spatial relations modulated by the scope of attention, revealed a pattern of causal connectivity that changed during the different phases of the task. This pattern is in line with the proposed theory of a hemispheric specialization of spatial relation processing (e.g. CAT, left hemisphere; and COO, right hemisphere) as well as predictions, derived from theory, about the benefits of manipulating the scope of the attention window (e.g. CAT, small cue; and COO, large cue) on specific types of spatial relation processing (van der Ham *et al.*, 2014). The present analysis also revealed a key causal role of the middle frontal gyrus towards parietal and visual cortices for both spatial relation judgments. Most probably, the middle frontal gyrus may implement a mechanism originally posited by Kosslyn (1994, pp. 230–233) in his neural architecture of spatial relation processing. In his model, Kosslyn reasoned that a specific neural system converts all spatial information, including categorical relations, into coordinates (i.e. information about the size, distance and orientation of the object currently being viewed) so as to guide top-down search. Such a mechanism would be relevant also for shifting top-down attention to compute categorical spatial relations, as categorical spatial relations correspond to a range of locations and this cannot be used to shift attention directly to a correct location (e.g. the head and paws of an animal).

GC, a statistical method for estimating the directional causal influence among different sources, plays a key role in understanding cerebral functions in normal participants (Gow *et al.*, 2008; Ge *et al.*, 2009, 2012; Luo *et al.*, 2011) as well as in patients (Miao *et al.*, 2011; Franciotti *et al.*, 2013b), providing directed functional connectivity maps (Barrett & Barnett, 2013).

Generally, it is difficult to establish a universal pattern of the dynamics of activity propagation during a task performance, as there is a large inter-subject variability connected with the different RTs and different strategies in solving the task; however, some general trends can be observed (Blinowska *et al.*, 2010).

In our paradigm, GC analysis was used to estimate the causal connectivity across brain areas for selected time intervals. Differently from other analysis methodologies such as correlation or coherencem which highlight the functional connectivity among brain areas, GC has the advantage that it estimates the causal direction of information flow between areas, revealing which area sends and which area receives information. Knowledge of the direction of causal information is related to the specific time interval under scrutiny, but it is not possible to infer how long the exchange lasts and, in particular when the exchange is bi-directional, it is not possible to establish which direction starts first. Moreover, GC does not allow us to estimate in which way the signal source influences the sink, for example if the source will evoke an increment or a decrement of the intensity of the receiving signal, but it allows us to explicitly quantify an underlying causal mechanism. In addition, MVAR models can be applied to stationary signals, and thus these approaches have the disadvantage that the non-stationary contribution to the signals has to be removed. A widely used strategy to generate the covariance stationarity is to apply the first-order differencing to time series (Seth, 2005, 2010; Gow *et al.*, 2008).

However, this procedure may complicate the interpretation, as what is being assessed is the causal connectivity among changes in each time series.

New approaches such as adaptive MVAR models (Hesse *et al.*, 2003; Astolfi *et al.*, 2008) that make no assumptions about the stationarity of the signals or information theoretic tools, such as transfer entropy (Schreiber, 2000), a model-free method that measures directed non-linear and linear information flow have been proposed and applied successfully to simulated and real electrophysiological data (Vicente *et al.*, 2011; Plomp *et al.*, 2014). Future studies with new statistical approaches should attempt to determine the effective functional mechanisms that underlie the observed data.

Acknowledgements

The authors declare that the research was conducted in the absence of any commercial or financial relationships that could be construed as a potential conflict of interest.

Abbreviations

ANOVA, analysis of variance; CAT, categorical; COO, coordinate; ECD, equivalent current dipole; GC, Granger causality; LIPL, left inferior parietal lobe; LMFG, left middle frontal gyrus; LORETA, low-resolution brain electromagnetic tomography analysis; LSPL, left superior parietal lobe; LVC, left visual cortex; MEG, magnetoencephalography; MRI, magnetic resonance imaging; NoCh, 'no change'; RIPL, right inferior parietal lobe; RMFG, right middle frontal gyrus; ROI, region of interest; RSPL, right superior parietal lobe; RT, reaction time; RVC, right visual cortex; VAR, vector autoregressive.

References

Akaike, H. (1974) A new look at the statistical model identification. *IEEE T. Automat. Contr.*, **19**, 716–723.

Amorapanth, P.X., Widick, P. & Chatterjee, A. (2010) The neural basis for spatial relations. *J. Cognitive Neurosci.*, **22**, 1739–1753.

Astolfi, L., Cincotti, F., Mattia, D., De Vico Fallani, F., Tocci, A., Colosimo, A., Salinari, S., Marciani, M.G., Hesse, W., Witte, H., Ursino, M., Zavaglia, M. & Babiloni, F. (2008) Tracking the time-varying cortical connectivity patterns by adaptive multivariate estimators. *IEEE T. Bio-Med. Eng.*, **55**, 902–913.

Baccalà, L.A. & Sameshima, K. (2001) Partial directed coherence: a new concept in neural structure determination. *Biol. Cybern.*, **84**, 463–474.

Baciu, M., Koenig, O., Vernier, M.P., Bedoin, N., Rubin, C. & Segebarth, C. (1999) Categorical and coordinate spatial relations: fMRI evidence for hemispheric specialization. *NeuroReport*, **10**, 1373–1378.

Barrett, A.B. & Barnett, L. (2013) Granger causality is designed to measure effect, not mechanism. *Front. Neuroinform.*, **7**, 6.

Benjamini, Y. & Hochberg, Y. (1995) Controlling the false discovery rate: a practical and powerful approach to multiple testing. *J. Roy. Stat. Soc. B.*, **57**, 289–300.

Blinowska, K., Kus, R., Kaminski, M. & Janiszewska, J. (2010) Transmission of brain activity during cognitive task. *Brain Topogr.*, **23**, 205–213.

Bressler, S.L. & Seth, A.K. (2011) Wiener–Granger causality: a well established methodology. *NeuroImage*, **58**, 323–329.

Bunge, S.A., Ochsner, K.N., Desmond, J.E., Glover, G.H. & Gabrieli, J.D. (2001) Prefrontal regions involved in keeping information in and out of mind. *Brain*, **124**, 2074–2086.

Corbetta, M. & Shulman, G.L. (2002) Control of goal-directed and stimulus-driven attention in the brain. *Nat. Rev. Neurosci.*, **3**, 201–215.

Corbetta, M., Akbudak, E., Conturo, T.E., Snyder, A.Z., Ollinger, J.M., Heather, A.D., Linenweber, M.R., Petersen, S.E., Raichle, M.E., Van Essen, D.C. & Shulman, G.L. (1998) A common network of functional areas for attention and eye movements. *Neuron*, **21**, 761–773.

Cui, J., Xu, L., Bressler, S.L., Ding, M. & Liang, H. (2008) BSMART: a Matlab/C toolbox for analysis of multichannel neural time series. *Neural Networks*, **21**, 1094–1104.

Della Penna, S., Del Gratta, C., Granata, C., Pasquarelli, A., Pizzella, V., Rossi, R., Russo, M., Torquati, K. & Erné, S.N. (2000) Biomagnetic systems for clinical use. *Philos. Mag. B.*, **80**, 937–948.

Della Penna, S., Torquati, K., Pizzella, V., Babiloni, C., Franciotti, R., Rossini, P.M. & Romani, G.L. (2004) Temporal dynamics of alpha and beta rhythms in human SI and SII after galvanic median nerve stimulation. A MEG study. *NeuroImage*, **22**, 1438–1446.

Desimone, R. & Duncan, J. (1995) Neural mechanisms of selective visual attention. *Annu. Rev. Neurosci.*, **18**, 193–222.

Ding, M., Bressler, S., Yang, W. & Liang, H. (2000) Short-window spectral analysis of cortical event-related potentials by adaptive multivariate autoregressive modeling: data preprocessing, model validation, and variability assessment. *Biol. Cybern.*, **83**, 35–45.

Franciotti, R., D'Ascenzo, S., Di Domenico, A., Onofrj, M., Tommasi, L. & Laeng, B. (2013a) Focusing narrowly or broadly attention when judging categorical and coordinate spatial relations: a MEG study. *PLoS One*, **8**, e83434.

Franciotti, R., Falasca, N.W., Bonanni, L., Anzellotti, F., Maruotti, V., Comani, S., Thomas, A., Tartaro, A., Taylor, J.P. & Onofrj, M. (2013b) Default network is not hypoactive in dementia with fluctuating cognition: an Alzheimer disease/dementia with Lewy bodies comparison. *Neurobiol. Aging*, **34**, 1148–1158.

Ge, T., Kendrick, K. & Feng, J. (2009) A novel extended granger causal model approach demonstrates brain hemispheric differences during face recognition learning. *PLoS Comput. Biol.*, **5**, e1000570.

Ge, T., Feng, J., Grabenhorst, F. & Rolls, E. (2012) Componential Granger causality, and its application to identifying the source and mechanisms of the top-down biased activation that controls attention to affective vs sensory processing. *NeuroImage*, **59**, 1846–1858.

Geweke, J. (1982) Measurement of linear dependence and feedback between multiple time series. *J. Am. Stat. Assoc.*, **77**, 304–313.

Gow, D.W., Segawa, J.A., Ahlfors, S.P. & Lin, F.H. (2008) Lexical influences on speech perception: a Granger causality analysis of MEG and EEG source estimates. *NeuroImage*, **43**, 614–623.

Granger, C.W.J. (1969) Investigating causal relations by econometric models and cross-spectral methods. *Econometrica*, **37**, 424–438.

van der Ham, I.J., Postma, A. & Laeng, B. (2014) Lateralized perception: the role of attention in spatial relation processing. *Neurosci. Biobehav. R.*, **45**, 142–148.

Hesse, W., Möller, E., Arnold, M. & Schack, B. (2003) The use of time-variant EEG Granger causality for inspecting directed interdependencies of neural assemblies. *J. Neurosci. Meth.*, **124**, 27–44.

Jiao, Q., Lu, G., Zhang, Z., Zhong, Y., Wang, Z., Guo, Y., Li, K., Ding, M. & Liu, Y. (2011) Granger causal influence predicts BOLD activity levels in the default mode network. *Hum. Brain Mapp.*, **32**, 154–161.

Kastner, S. & Ungerleider, L.G. (2000) Mechanisms of visual attention in the human cortex. *Annu. Rev. Neurosci.*, **23**, 315–341.

Kosslyn, S.M. (1987) Seeing and imagining in the cerebral hemispheres: a computational approach. *Psychol. Rev.*, **94**, 148–175.

Kosslyn, S.M. (1994) *Image and Brain: The Resolution of the Imagery Debate*. MIT Press, Cambridge, MA.

Kosslyn, S.M. & Jacobs, R.A. (1994) Encoding shape and spatial relations: a simple mechanism for coordinating complementary representations. In Honavar, V. & Uhr, L.M. (Eds), *Artificial Intelligence and Neural Networks: Steps Toward Principled Integration*. Academic Press, Boston, MA, pp. 373–385.

Kosslyn, S.M., Koenig, O., Barrett, A., Cave, C.B., Tang, J. & Gabrieli, J.D. (1989) Evidence for two types of spatial representations: hemispheric specialization for categorical and coordinate relations. *J. Exp. Psychol. Human.*, **15**, 723–735.

Kosslyn, S.M., Thompson, W.L., Gitelman, D.R. & Alpert, N.M. (1998) Neural systems that encode categorical versus coordinate spatial relations: PET investigations. *Psychobiology*, **26**, 333–347.

Laeng, B. (1994) Lateralization of categorical and coordinate spatial functions: a study of unilateral stroke patients. *J. Cognitive Neurosci.*, **6**, 189–203.

Laeng, B. (2006) Constructional apraxia after left or right unilateral stroke. *Neuropsychologia*, **44**, 1595–1606.

Laeng, B. (2013) Representation of spatial relations. In Ochsner, K. & Kosslyn, S.M. (Eds), *The Oxford Handbook of Cognitive Neuroscience, Volume I, Core Topics*. Oxford University Press, Oxford, pp. 28–59.

Laeng, B., Carlesimo, G.A., Caltagirone, C., Capasso, R. & Miceli, G. (2002) Rigid and non-rigid objects in canonical and non-canonical views: hemisphere-specific effects on object identification. *Cogn. Neuropsychol.*, **19**, 697–720.

Laeng, B., Okubo, M., Saneyoshi, A. & Michimata, C. (2011) Processing spatial relations with different apertures of attention. *Cognitive Sci.*, **35**, 297–329.

Luo, Q., Ge, T. & Feng, J. (2011) Granger causality with signal-dependent noise. *NeuroImage*, **57**, 1422–1429.

Miao, X., Wu, X., Li, R., Chen, K. & Yao, L. (2011) Altered connectivity pattern of hubs in default-mode network with Alzheimer's disease: an Granger causality modeling approach. *PLoS One*, **6**, e25546.
Michimata, C., Saneyoshi, A., Okubo, M. & Laeng, B. (2011) Effects of global and local attention on the processing of categorical and coordinate spatial relations. *Brain Cognition*, **77**, 292–297.
Moore, T., Armstrong, K.M. & Fallah, M. (2003) Visuomotor origins of covert spatial attention. *Neuron*, **40**, 671–683.
Okubo, M., Laeng, B., Saneyoshi, A. & Michimata, C. (2010) Exogenous attention differentially modulates the processing of categorical and coordinate spatial relations. *Acta Psychol.*, **135**, 1–11.
Pascual-Marqui, R.D., Esslen, M., Kochi, K. & Lehmann, D. (2002) Functional imaging with low-resolution brain electromagnetic tomography (LORETA): a review. *Method. Find. Exp. Clin.*, **24**, 91–95.
Plomp, G., Quairiaux, C., Michel, C.M. & Astolfi, L. (2014) The physiological plausibility of time-varying Granger-causal modeling: normalization and weighting by spectral power. *NeuroImage*, **97C**, 206–216.
Rosen, A.C., Rao, S.M., Caffarra, P., Scaglioni, A., Bobholz, J.A., Woodley, S.J., Hammeke, T.A., Cunningham, J.M., Prieto, T.E. & Binder, J.R. (1999) Neural basis of endogeneous and exogeneous spatial orienting: a functional MRI study. *J. Cognitive Neurosci.*, **11**, 135–152.
Samonas, M., Petrou, M. & Ioannides, A.A. (1997) Identification and elimination of cardiac contribution in single-trial magnetoencephalographic signals. *IEEE T. Bio-Med. Eng.*, **44**, 386–393.
Schelter, B., Winterhalder, M., Eichler, M., Peifer, M., Hellwig, B., Guschlbauer, B., Lücking, C.H., Dahlhaus, R. & Timmer, J. (2005) Testing for directed influences among neural signals using partial directed coherence. *J. Neurosci. Meth.*, **152**, 210–219.
Schreiber, T. (2000) Measuring information transfer. *Phys. Rev. Lett.*, **85**, 461–464.
Serences, J.T. & Yantis, S. (2006) Selective visual attention and perceptual coherence. *Trends Cogn. Sci.*, **10**, 38–45.
Seth, A.K. (2005) Causal connectivity of evolved neural networks during behavior. *Network-Comp. Neural.*, **16**, 35–55.
Seth, A.K. (2010) A MATLAB toolbox for Granger causal connectivity analysis. *J. Neurosci. Meth.*, **186**, 262–273.
Slotnick, S.D. & Moo, L.R. (2006) Prefrontal cortex hemispheric specialization for categorical and coordinate visual spatial memory. *Neuropsychologia*, **44**, 1560–1568.
Slotnick, S.D., Moo, L.R., Tesoro, M.A. & Hart, J. (2001) Hemispheric asymmetry in categorical versus coordinate visuospatial processing revealed by temporary cortical deactivation. *J. Cognitive Neurosci.*, **13**, 1088–1096.
Trojano, L., Grossi, D., Linden, D.E., Formisano, E., Goebel, R., Cirillo, S., Elefante, R. & Di Salle, F. (2002) Coordinate and categorical judgements in spatial imagery. An fMRI study. *Neuropsychologia*, **40**, 1666–1674.
Trojano, L., Conson, M., Maffei, R. & Grossi, D. (2006) Categorical and coordinate spatial processing in the imagery domain investigated by rTMS. *Neuropsychologia*, **44**, 1569–1574.
Vicente, R., Wibral, M., Lindner, M. & Pipa, G. (2011) Transfer entropy – a model-free measure of effective connectivity for the neurosciences. *J. Comput. Neurosci.*, **30**, 45–67.
Yoo, K., Sohn, W.S. & Jeong, Y. (2013) Tool-use practice induces changes in intrinsic functional connectivity of parietal areas. *Front. Hum. Neurosci.*, **7**, 49.